

An Efficient One-Dimensional Fractal Analysis for Iris Recognition

Chuan Chin Teo
Faculty of Information Technology
Multimedia University
Jalan Multimedia, 63100,
Cyberjaya, Selangor, Malaysia
ccteo@mmu.edu.my

Hong Tat Ewe
Faculty of Information Technology
Multimedia University
Jalan Multimedia, 63100,
Cyberjaya, Selangor, Malaysia
htewe@mmu.edu.my

ABSTRACT

An iris recognition system is proposed in this paper. This system implements (a) the combination of proposed black hole search method and integro-differential operators for iris localization, (b) one-dimensional fractal analysis for feature extraction and (c) dissimilarity operator for matching. The black hole search method achieves 100% accuracy of pupil detection for both CASIA and MMU Iris databases. Experiment results show that the proposed system has an encouraging result with low EER to 4.63% in CASIA iris database and 4.17% in MMU iris database. It provides an alternative solution for iris recognition and acts as a spring board for further investigation.

Keywords

Black hole Search, 1-D Fractal Dimension, Dissimilarity Operator.

1. INTRODUCTION

The latest threats of security have led to increased awareness of biometric technologies. Biometric, in general terms, is defined as automated personal identification or authentication based on a physiological and behavioural characteristics [Tis02a]. Fingerprint-based authentication is the most widely accepted and mature biometric, dominating the majority of commercial, civilian, and law enforcement markets. However, it requires physical contact with scanner, and dirt on the finger can affect the recognition.

Recently, iris-based authentication presents promising results for biometric technologies. The iris, as showed in Figure 1, has rich and unique

patterns of striations, pits, coronas, freckles, fibers, filaments, furrows, rifts, rings, and vasculature. As reported in Daugman [Dau95a] the uniqueness of every iris parallels the uniqueness of every fingerprint, but owns further practical advantages over fingerprint and other biometrics. This indicates that no two irises are indistinguishable and that the chance of finding two people with identical iris pattern is almost zero [Tis02a], [Bo98a]. Furthermore, the iris pattern is stable throughout life and can be noninvasive authenticated due to its externally visible behaviour [Ma03a]. These advantages make it a promising solution to security and commercial applications.

In this paper, we propose a novel analysis for an iris recognition system based on one-dimensional fractal dimension. The rest of this paper is structured as follows. Section 2 contains a complete account of the overall process of proposed system. Experimental results are displayed in section 3.

Permission to make digital or hard copies of all or part of this work for personal or classroom use is granted without fee provided that copies are not made or distributed for profit or commercial advantage and that copies bear this notice and the full citation on the first page. To copy otherwise, or republish, to post on servers or to redistribute to lists, requires prior specific permission and/or a fee.

WSCG SHORT papers, ISBN 80-903100-9-5
WSCG'2005, January 31-February 4, 2005
Plzen, Czech Republic.
Copyright UNION Agency – Science Press

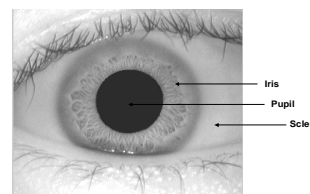


Figure 1. Sample of iris image

2. Iris-based Authentication System

This section describes an overview of all fundamental processes in our iris recognition system. These processes are generally referred to as image acquisition, image preprocessing, feature extraction and matching, respectively.

2.1 Image Acquisition

We are using the iris image database from CASIA Iris Image Database [CAS03a] and MMU Iris Database [MMU04a]. CASIA Iris Image Database contributes a total number of 756 iris images which were taken in two different time frames. Each of the iris images is 8-bit gray scale with a resolution of 320x280. Details of iris image acquisition technique can be referred from [Ma03a]. Nevertheless, MMU Iris Database contributes a total number of 450 iris images which were captured by LG IrisAccess@2200.

2.2 Iris Region Localization

Daugman's integro-differential operators [Dau95a] have been proven effective in iris localization. Our studies serve the dual purposes of gaining a broad understanding on integro-differential operators, and combining a new mathematical solution with it to improve the computational speed and reliability during localization process. For this reason, we introduce a combination of black hole search method and integro-differential operators for iris localization. Firstly, a black hole search method is proposed to detect the center of a pupil. For simple objects like circle and square, the center of mass is at the center of the object [Gre94a]. The center of mass refers to the balance point (x, y) of the object where there is equal mass in all directions [Gre94a]. Both the inner and outer iris boundaries can be taken as circles. Therefore, we can find the center of pupil by calculating its center of mass. The steps of black hole search method are as follows:

1. Find the darkest point of image (referred as black hole) in the global image analysis.
2. Determine a range of darkness (based on 1) designated as the threshold value (t) for identification of black holes.
3. Determine the number of black holes and their coordinates according to the predefined threshold. Calculate the center of mass of these black holes.
4. Construct a square region centered at the estimated center.
5. Repeat step 3 to improve the estimation of actual center of pupil.

The black holes represent the pixels exist within the interior of the pupil. Similarly, the total number of black holes represents the area of the pupil. In Equation 1, E_x denotes the estimated center

coordinate- x and E_y denotes the estimated center coordinate- y from the global image analysis, where W and H represent the sum of detected coordinate- x and coordinate- y which satisfy $I(x, y) < t$ respectively.

$$E_x = \frac{\sum_{x=0}^{W-1} \sum_{y=0}^{H-1} x}{WH} \quad \text{if } I(x, y) < t;$$

$$E_y = \frac{\sum_{x=0}^{W-1} \sum_{y=0}^{H-1} y}{WH} \quad \text{if } I(x, y) < t \quad (1)$$

In order to acquire more accurate result, we repeat the steps and calculate the actual center of mass (C_x, C_y) from the local region analysis where a square window with side 60 centered at E_x, E_y is chosen for the analysis. Equation 2 defines the actual center of the pupil, and w and h represent the sum of detected coordinate- x and coordinate- y which satisfy $I(x, y) < t$ in predefined region respectively.

$$C_x = \frac{\sum_{x=E_x-L}^{E_x+L} \sum_{y=E_y-L}^{E_y+L} x}{wh} \quad \text{if } I(x, y) < t;$$

$$C_y = \frac{\sum_{x=E_x-L}^{E_x+L} \sum_{y=E_y-L}^{E_y+L} y}{wh} \quad \text{if } I(x, y) < t \quad (2)$$

In Equations 1 and 2, t is the threshold value and $I(x, y)$ is the image intensity. CASIA iris images are captured by near-infrared illumination sensor. Therefore, they have no reflected spot on the pupil. In contrast, MMU iris images are captured by non-intrusive illumination and have less reflected spot on the pupil. As a result, the proposed algorithm is very effective for both CASIA and MMU iris database. Furthermore, the radius can be calculated from the given area (total number of black holes in the pupil), where

$$Radius = \sqrt{\frac{Area}{\pi}} \quad (3)$$

In order to complete the iris localization process, a Gaussian smoothing is used to filter out the high frequency noise of the image. Next, the outer boundary of an iris can be detected by using integro-differential operators [Dau95a]. This method is found to be efficient and effective in CASIA and MMU iris images as well. Figure 2 shows the detected inner and outer boundary of an iris. At the same time, the localized iris region is positioned into rectangular iris template.

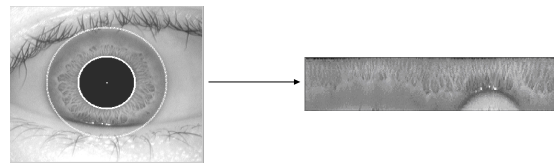


Figure 2. Sample iris after localization

2.3 Image Normalization

An iris has the function of controlling the light entering into the eye by adjusting the size of pupil. Consequently, it causes the elastic deformation in iris image. On the other hand, the size of iris image can be inconsistent due to different distance between the iris and camera.

Thus, it is important to normalize the iris image into a standard size (87x360) using interpolation technique. Figure 3 shows the normalized template of an iris.



Figure 3. Sample iris after normalization

2.4 Feature Extraction

Fractal geometry can intuitively be thought as irregular geometric representation in human's iris. Thus, the fractal information can be used to illustrate an iris. In fact, the fractal information from a multi-dimensional image can be calculated by constructing it into three-dimensional representation [Low99a], where the additional h-axis is represented by its gray levels. On the other hand, the unique details of the iris generally spread along the angular direction which corresponds to the variation of pattern in vertical direction [Ma04a]. Owing to the two fundamental properties above, we use one dimensional fractal analysis to generate a structured feature vector for an iris.

The earliest step in fractal analysis endeavor is to normalize all the pixels from the preprocessed iris. The gray level value of $I(x, y, h)$ for all pixels in the iris template is normalized according to Equation 4.

$$I(x, y, h) = I(x, y, h) \times \frac{L}{H} \quad (4)$$

where the L is the appropriate window size and H is the maximum value of gray level.

In advance, the pixels within each row along the angular direction are positioned into an appropriate square with L x L window size. This pixel allocation process is illustrated in Figure 4.

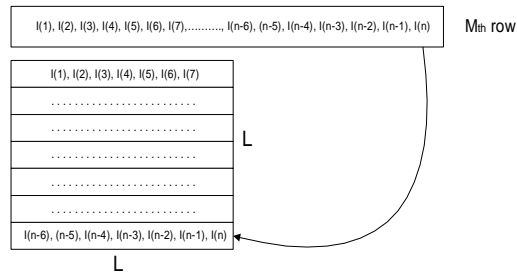


Figure 4. Pixel allocation with L x L window size

Next, a surface coverage method [Ewe93a] is performed to calculate the fractal dimension.

The fractal dimension [Sch91a] is defined as:

$$D = \frac{\log(N)}{\log(1/r)} \quad (5)$$

where N is the number of scaled down copies (difference of dimension between neighboring pixels within a box) of the original object which is needed to fill up the original object and $r = 1/L$. Consequently, each row of the iris template will produce the fractal information and form a structured feature vector (f) for particular iris.

$$f = \{D_1, D_2, D_3, \dots, D_{m-3}, D_{m-2}, D_{m-1}, D_m\} \quad (6)$$

where D_m is the fractal information of mth row in a iris template. In feature extraction stage, we generate 87 features to illustrate an iris code. This record is saved in a database for further comparison.

The approach mentioned above has fast computational speed and less memory usage due to the compression of a list of circular data into a single fractal feature. Moreover, it achieves rotational invariant as the 1-D feature represents the whole circular data.

2.5 Matching

In the matching phase, a simple dissimilarity operator is proposed to compare a pair of iris code. The steps of formulating the dissimilarity operator are described as follows:

1. Initialize a tolerance threshold. In our case, we use $Tt (= 0.0025)$.
2. Compute the absolute differences between default feature vector (D1) and current feature vector (D2).
3. Increase the number of occurrence for every absolute feature-by-feature differences that exceeds tolerance threshold through accumulator
4. Calculate the average dissimilarity between two feature vectors.

The equation of our dissimilarity operator can be expressed as:

$$\text{Average Dissimilarity} = \frac{1}{87} \sum_{i=1}^{87} |D1_i - D2_i|$$

$$\text{if } |D1_i - D2_i| > Tt \quad (7)$$

where D1 is the default feature vector, D2 is current feature vector and Tt is the tolerance threshold. In real application, the average dissimilarity equal to zero seldom happens. Therefore, the algorithm to select a good match is based on average dissimilarity

which is nearest to zero and falls below a predefined threshold (t).

3. Experiment Results

The proposed black holes search method proves its ability to detect inner boundary of the iris. It exhibits 100% success of pupil detection for both CASIA and MMU Iris databases. Figure 7 shows the actual results of black hole search method.

On the other hand, integro-differential operators work properly on both CASIA and MMU iris database for outer iris detection. However, the failure may occurs due to low contrast, eyelids and eyelashes occlusion. The probability of failure on outer iris detection is around 2% in CASIA and MMU iris database.

The experiment was continued to validate the performance of proposed algorithm. In verification procedure, the False Reject Rate (FRR), False Accept Rate (FAR) and Equal Error Rate (EER) tests were computed in both databases, where Figure 5 and Figure 6 shows the results of CASIA and MMU iris datasets respectively. Accordingly, EER is calculated from the ROC curve. The EER is the point on the ROC curve where the FAR is equal to the FRR. In our experiment on CASIA iris database, the EER is approximately 4.63 %. Nevertheless, MMU iris database has lower EER which is 4.17%.

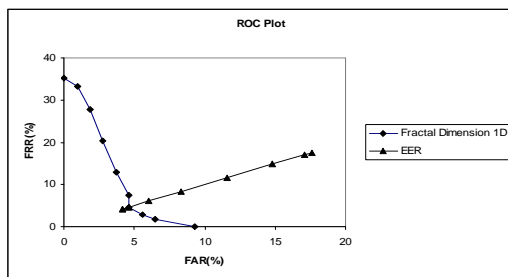


Figure 5. ROC plot for CASIA iris database

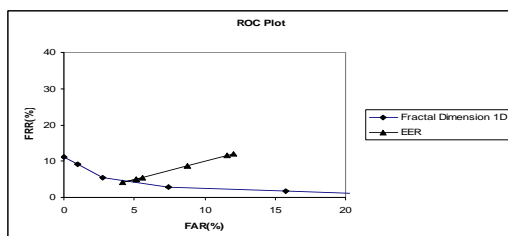


Figure 6. ROC plot for MMU iris database

4. Acknowledgement

This work was supported by Malaysia IRPA (Intensified Research in Priority Areas) funding. The authors wish to thank Institute of Automation, Chinese Academy of Sciences for providing CASIA iris database.

5. Reference

- [Tis02a] Tisse, C., Martin, L., Torres, L. and Robert, M. (2002): Person Identification Technique using Human Iris Recognition. In Proc, Vision Interface, pp. 294-299.
- [Dau95a] Daugman, J. (1995): High Confident Personal Identification by Rapid Video Analysis of Iris Texture. In Proc, European Convention on Security and Detection, pp. 244-251.
- [Bo98a] Boles, W. and Boashash, B. (1998): A Human Identification Technique Using Images of the Iris and Wavelet Transform, IEEE Trans. Signal Processing, vol 46, no.4, pp. 1185-1188.
- [Ma03a] Ma L., Tan T., Wang Y. and Zhang, D. (2003): Personal Identification Based on Iris Texture Analysis. IEEE Trans. PAMI, vol 25, no.12, pp. 1519-1533.
- [Ma04a] Ma L., Tan T., Wang Y. and Zhang, D. (2004): Efficient Iris Recognition by characterizing Key Local Variations, IEEE Trans. Image Processing, vol 13, no.6, pp. 739-750.
- [Low99a] Low, H.K., Chuah, H.T and Ewe, H.T. (1999): A Neural Network Landuse Classifier for SAR Images using Texture and Fractal Information, in Proc. Geocarto International, vol. 14, no.1, pp. 67-74.
- [Gre94a] Gregory A., B. (1994): Digital Image Processing: Principles and Applications, Wiley.
- [CAS03a] CASIA Iris Image Database (version 1.0): Institute of Automation (IA), Chinese Academy of Sciences (CAS), <http://www.sinobiometrics.com>
- [MMU04a] MMU Iris Image Database: Multimedia University, <http://pesona.mmu.edu.my/~ccteo/>
- [Ewe93a] Ewe, H.T., Au, W.C., Shin, R.T. and Kong, J.A. (1993): Classification of SAR Images Using a Fractal Approach, in Proc. Electromagnetic Research Symposium, pp. 493.
- [Sch91a] Schroeder, M.R. (1991): Fractal, Chaos, Power Laws: Minutes from an Infinite Paradise, Freeman.